Proceedings of the 2022 IEEE
International Conference on Robotics and Biomimetics
December 5-9, 2022, Xishuangbanna, China

Design of an Intelligent Robot for Back-Slap Sputum Excretion Based on Back Feature Recognition

Diansheng Chen, Yue Pan, Yuanhai Huang, Min Wang*, Renren Bao and Chunxia Tang

***Abstract*— Under the circumstance of COVID-19 epidemic spread, global medical resources are in serious shortage. As a common way of care for respiratory diseases, although back-slap sputum excretion can be used for the care of lung diseases, but it requires the cooperation of multiple medical staff, and lead to inefficient care. This paper designed a method of the human`s back feature recognition based on YOLOv5, and built a new type of intelligent robot for back-slap sputum excretion on this basis, which can assist care staff to complete the back-slap sputum excretion care for patients, and reduce the labor intensity of staff and the risk of cross infection.**

***Keywords*— intelligent robot; back-slap sputum excretion; feature recognition.**

I. INTRODUCTION

Currently, the global COVID-19 epidemic is persistently raging and the medical resources are in severe shortage. According to the latest information released by the World Health Organization, the number of confirmed cases of COVID-19 epidemic worldwide has reached 600 million[1]. Many hospitals treating respiratory illnesses by back-slap to sputum excretion, including COVID-19. This method requires paramedics to slap the patients' back from bottom to top and from outside to inside while holding their hand as an empty palm, and then assist the patients to expectoration by physical means[2]. During the operation, the care staff need to avoid the scapula and spine in order to prevent secondary injury to the patient. The area where back-slap sputum excretion operation can be performed is shown in Figure1, the green part is the area that can be slapped, and the red area is the scapula and spine that need to be avoided.

Figure 1. Back-slap sputum excretion area.

The manual back-slap sputum excretion operation generally requires 2-3 care staff`s cooperation to carry out various tasks, including patient turning over, maintain body position and back-slap. However, the work efficiency of this method is low, and the distance between care staff and patients is close, which increases the risk of doctor-patient cross infection. In the past few decades, the service robot industry has developed rapidly. IFR (International Federation of Robotics) predicted that the total global output value of service robots in 2023 would reach 12.1 billion US dollars[3]. To reduce the labor intensity of care staff, service robots have also been applied in medical scenarios. In the context of this research, we developed an intelligent robot for back-slap sputum excretion, which can effectively recognize the features of patients' back, using the feature`s information to plan the movement trajectory of the back-slap sputum excretion terminal, and then used the terminal equipped with the robotic arm to realize the back-slap sputum excretion care for critically ill patients.

At present, there are many studies on the recognition of the human`s back features to realize the imitation motion of the human`s back. Current research on back feature recognition mainly focuses on massage robots and bathing robots. Harbin Engineering University and Beihang University had jointly developed a traditional Chinese medicine massage robot[4]. Although it can recognize the features of users' backs by recognizing the markers on users' clothes, the operation of this robot is relatively complex. Meanwhile, Shandong Architecture University had also developed a traditional Chinese medicine massage robot, as shown in Figure2(b). This robot could recognize the users' back features by pasting color markers on the back[5][6], but the limitation of this study was treating the human`s body as a plane. A study from National Taiwan University used RGB-D cameras to collect the human`s back information in 2014[7], it can effectively reconstruct the human`s back and estimate the posture of the human body to realize the feature recognition of the back. However, this study cannot distinguish the details of the back well. Moreover, the National Technical University of Athens &Greece also designed a bathing robot from 2016 to 2018 [8][9][10], it used the Kinect depth camera to collect 3D information on the back, and developed an algorithm to fuse

*Resrach supported by the National Key Research & Development Program of China (2021YFC0122700).

Diansheng Chen is with the Changsha Social Work College, Changsha, Hunan, China. And he is with the School of Mechanical Engineering and Automation, Beihang University, Beijing, China (e-mail: chends@163.com).

Yue Pan is with the School of Mechanical Engineering and Automation, Beihang University, Beijing, China (e-mail: panyue@buaa.edu.cn).

Yuanhai Huang is with the School of Mechanical Engineering and Automation, Beihang University, Beijing, China (e-mail: huangyh@buaa.edu.cn).

*Corresponding author: Min Wang is with the School of General Engineering, Beihang University, Beijing, China (phone: 18810283860; e-mail: wangmincc@163.com).

Renren Bao is with the SIASUN Robot & Automation CO., Ltd., Shenyang, Liaoning, China (e-mail: baorenren@siasun.com).

Chunxia Tang is with the Changsha Social Work College, Changsha, Hunan, China (e-mail: 961909529@qq.com).

2022 IEEE International Conference on Robotics and Biomimetics (ROBIO) | 978-1-6654-8109-0/22/$31.00 ©2022 IEEE | DOI: 10.1109/ROBIO55434.2022.10011775

combine 2D images and 3D point clouds as the basis for trajectory planning of a robotic arm equipped with a shower head. However, this robot mainly extracted the contour of the back edge, and its ability to recognize the feature`s information on the inside of the back is poor. In 2018, the University of Science and Technology of Ho Chi Minh City, Vietnam, proposed a massage robot using two parallel robotic arms[11]. This robot also used a depth camera to recognize the human`s back information, but it is limited to the recognition of the contour of the back edge.

The back feature recognition in existing research is just simply extracting the back contour which does not meet the specific needs of the intelligent robot for back-slap sputum excretion in actual usage. Therefore, this paper designed a back feature recognition method based on the marked points in space by fusing the 2D image with the 3D point cloud to ensure the accuracy of the back feature recognition. After the patients' back features are effectively recognized, the robot arm's end trajectory could be used to realize the automatic back-slap sputum excretion care of the patients, and then reduce the paramedics' workload and their risk of cross-infection.

The following chapters of this paper are organized as below: the second chapter would introduce the structure of the robot we designed, the third chapter would introduce the back feature recognition method designed by this research institute, the fourth chapter would introduce the motion planning of the intelligent robot for back-slap sputum excretion, the fifth chapter would conduct field experiments on the intelligent robot for back-slap sputum excretion, and the sixth chapter would summarize the full paper.

II. ROBOT STRUCTURE

A. Robot Structure Design

In terms of the overall structure design, the intelligent robot for back-slap sputum excretion would use an industrial computer as the core to directly control the Kinect and the robotic arm, and use Arduino as the underlying controller to control the back-slapping expectoration terminal. Serial ports are used for communication between the various components of the test platform. Figure 2 is the schematic diagram of the structure of the robot.

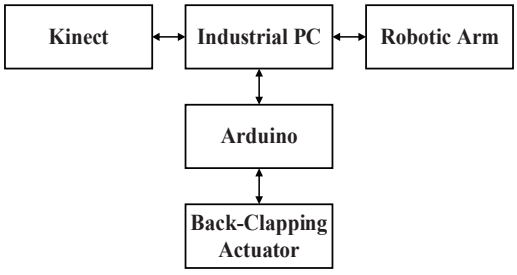

Figure 2. Schematic diagram of the robot.

In terms of the actual robot construction, the industrial computer is a PC computer equipped with the ubuntu18.04 system. We use the Microsoft Azure Kinect DK camera as a depth camera. The minimum depth can be measured is 0.25 meters which is suitable for the use of the intelligent robot for back-slap sputum excretion scenario. Meanwhile, we use the robotic arm (AUBO-C5 collaborative robot) with a maximum load of 5KG at the end a wingspan of 1008mm. And flexible working space with a diameter of 886.5mm which can meet the realistic needs. To meet the requirements of back-slap sputum excretion operation on the patients' back, we equip the robotic arm with a back-slap sputum excretion terminal at the end of it. Figure 3 is the physical map of our robot.

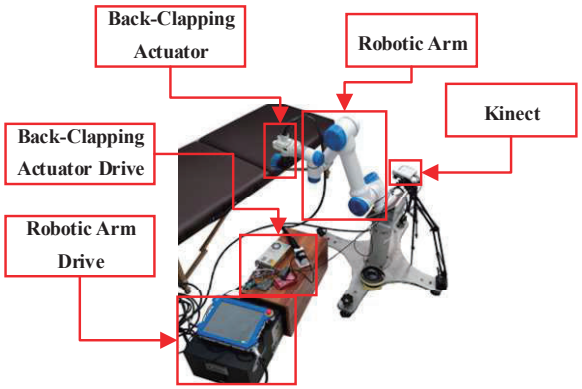

Figure 3. Physical map of the robot.

Here, we use Yangkun YK500 as back-slap sputum excretion terminal. The main principle of this kind of machine is to make direct contact with the human`s back, and then to achieve efficient beating on the back of the patient through the vibration of the terminal, and finally achieve the effect of shaking the sputum from the trachea.

B. End Clamp Design of Robotic Arm

Because the back-slap sputum excretion terminal is accompanied by large vibration during work, it is necessary to design a vibration reduction mechanism between the end flange of the robotic arm and the back-slap sputum excretion terminal. The robotic arm can be prevented from being disturbed by this method during working. Here we adopted the form of passive vibration reduction to dissipate vibration in the form of heat energy through a rubber damper, so as to reduce the influence of vibration generated by the back-slap sputum excretion terminal on the robotic arm. In order to achieve this purpose, firstly, we designed a special clamp to hold the back-slap sputum excretion terminal, and ensure the stability of the back-slap sputum excretion terminal through friction. Secondly, we designed a supporting platform between the back-slap sputum excretion terminal clamp and the end of the robotic arm, and installed a rubber damper between the supporting platform and the clamp. Figure 4 is the schematic diagram of the robotic arm end clamp.

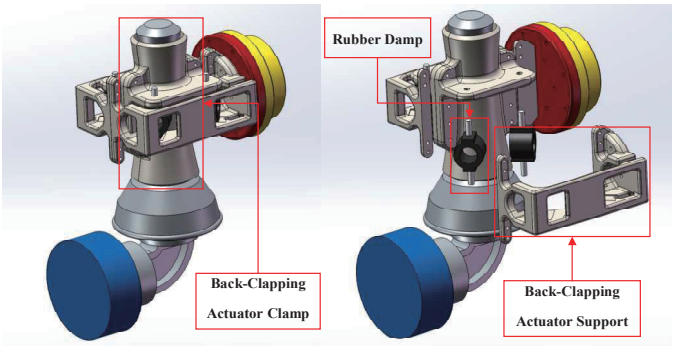

Figure 4. Schematic diagram of the robotic arm end clamp.

Figure 5 is the physical map of the robotic arm end clamp used in the robot designed in this paper.

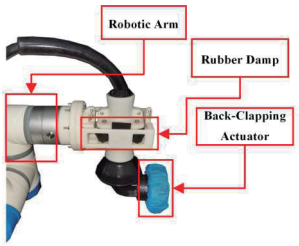

Figure 5. Physical map of the robotic arm end clamp.

III. BACK FEATURE RECOGNITION

When performing feature recognition on the human`s back, we first use markers to mark the features of the back. In this method, the markers are firstly pasted on the human`s back, and then use camera to collect the 2D visual image information of the human`s back. Here we design a marker recognition method based on YOLOv5. First, we identify the markers on the human`s back, and then perform point cloud registration on the 2D image and the 3D point cloud, and finally realize the extraction of the human`s back features.

A. 3D Visual Perception

In order to perform pixel-level recognition of the markers in the collected RGB images, we choose to use YOLOv5 as the main image recognition algorithm here. YOLOv5 is a regression-based multi-target detection algorithm, which can identify multiple different types of targets on the image, and it will automatically fit the external dimensions of the items and identify them with frame lines[12]. Figure 6 is a schematic diagram of the YOLOv5`s basic structure.

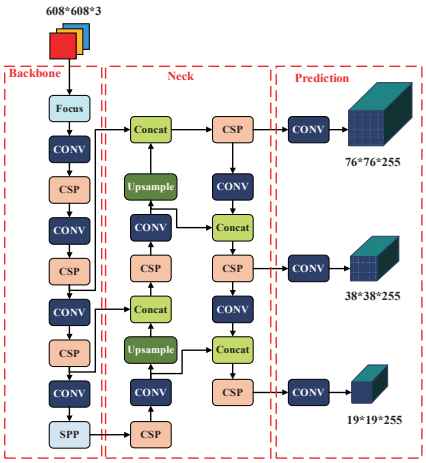

Figure 6. Schematic diagram of the YOLOv5`s basic structure.

YOLOv5 mainly includes 4 versions: YOLOv5l, YOLOv5m, YOLOv5, YOLOv5x. Among them, YOLOv5s is the basic version of the algorithm, and other versions have been broadened to a certain extent, so it is relatively smaller and faster in reasoning than other models. Considered the accuracy, efficiency and size of the recognition model, we finally selected YOLOv5s as the makers recognition algorithm. After the model is repeatedly trained, it can be used to identify the makers on the human`s back. Figure 7(a) is the recognition result of the makers on the back in the sitting posture state, and Figure 7(b) is the recognition result of the makers on the back in the lying posture state.

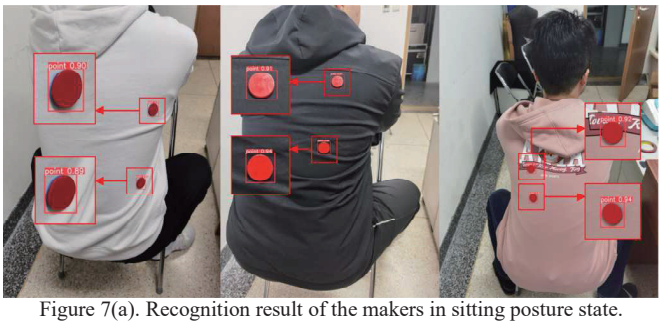

Figure 7(a). Recognition result of the makers in sitting posture state.

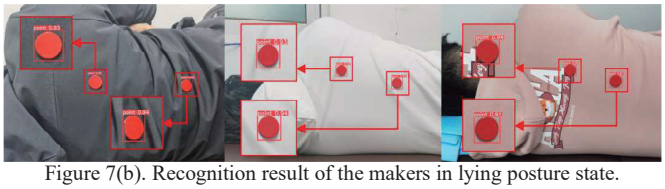

Figure 7(b). Recognition result of the makers in lying posture state.

On our test dataset, the IoU of the trained model is 0.9081, and the accuracy of the detection results can meet our actual use requirements; at the same time, all the required markers are effectively detected. It can be seen from the results that the trained YOLOv5s can effectively select the makers pasted on the human`s back, then the center point of the makers can be obtained through the calculation.

Here, we also tested the use of image thresholding to find the markers on human`s back. However, due to the change of illumination, this method has a large recognition error. At the same time, it is necessary to perform edge detection when using image threshold segmentation recognition, but from the actual test, we found that due to the marker`s pose and occlusion problem, it is difficult to ensure that the edge of the marker is circular during edge detection, which will make the marker cannot be detected correctly.

Next, in order to achieve effective slapping on the human`s back, the end of the robotic arm needs to move in the space required by the care staff. The back-slap sputum excretion terminal mounted on the robotic arm takes the makers pasted on the back as the starting point and the end point. In the previous section, we obtained the plane coordinates of the marked point in the 2D space of the RGB image, and then we need to fuse the RGB image with the 3D space point cloud to find the spatial coordinates of the makers, and thereby realize the robotic arm motion planning. In this research, we use Azure Kinect DK depth camera to collect in depth image information.

The result collected by Kinect DK is depth image. In order to realize the fusion of the RGB image and the point cloud, we need to align the RGB image and the depth image first. After that, when converting the point cloud, the image coordinate system needs to be converted into the world coordinate system, and the conversion needs to be completed in combination with the camera internal parameters. The conversion formula is shown in (1).

$$\begin{bmatrix} x \\ y \\ z \end{bmatrix} = D \begin{bmatrix} 1/f_x & 0 & 0 \\ 0 & 1/f_y & 0 \\ 0 & 0 & 1 \end{bmatrix} \begin{bmatrix} x` \\ y` \\ 1 \end{bmatrix} \quad (1)$$

The x, y, z are the coordinates under the point cloud coordinate system, $x`$, $y`$ are the coordinates under the image coordinate system, D is the depth value, and f_x, f_y are the camera internal parameters. The fused point cloud data is shown in Figure 8.

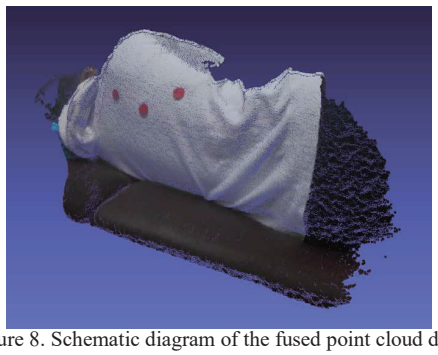

Figure 8. Schematic diagram of the fused point cloud data.

Based on the fused point cloud data results, the 3D coordinates of all points on the motion path of the back-slap sputum excretion terminal in space can be depicted.

B. Motion Track and Normal Generation

In the previous section, we have extracted the coordinates of the makers based on YOLOv5, and obtained the color point cloud data of the human`s entire back by fusing the RGB image and the point cloud data. In order to plan the motion path of the robotic arm, and at the same time to ensure that the back-slap sputum excretion terminal at the end of the robotic arm can fit the human`s back for continuous back-slap sputum excretion operations, it is necessary to obtain the 3D coordinates of the space points on the connection line between the multiple makers on back.

In the process of motion trajectory planning, we used the K-tree to filter the adjacent points of the motion trajectory. K-tree is mainly used to organize multi-dimensional data points, and the K-dimensional space is continuously divided by hyperplane to achieve fast retrieval of data. The structure diagram is shown in Figure 9. Each level of the K-tree would first use the maximum variance method or the sequential traversal method to formulate the structural division dimension, and then divide the multi-dimensional data according to this dimension. After that we would form a K-tree based on the construction of the binary tree according to the selected method [13].

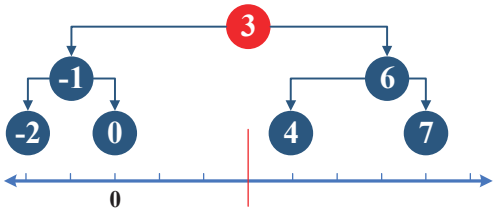

Figure 9. K-tree structure diagram.

The normal of the space point is equivalent to the normal of the tangent plane to this point, and the normal vector of the tangent plane is used as the vector of the point, that is, the least squares method can be used for plane fitting estimation. On this basis, PCA is used to estimate the plane, and the feature vector describing the plane can be obtained after data compression and dimension reduction, and the normal vector is one of them. Above that, the process of generating the trajectory normal is shown in Figure 10.

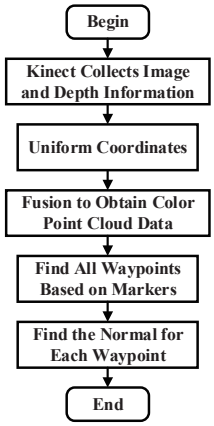

Figure 10. Flow chart of normal generation of trajectory.

Based on above analysis, the trajectory normal at the robotic arm end can be generated, and the result is shown in Figure 11.

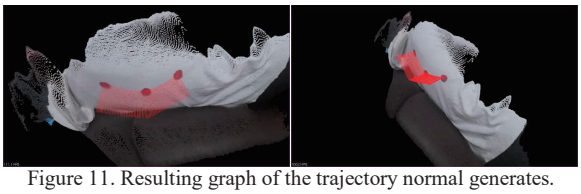

Figure 11. Resulting graph of the trajectory normal generates.

The normal generated here is a vector, and the starting point of the vector is the actual point of the point cloud data on the human`s back. When the end of the robotic arm is actually moving, the generated trajectory normal can be used to plan the end posture and perform the movement to make the back-slap sputum excretion terminal better fit the features of the human`s back.

IV. ROBOTIC ARM MOTION PLANNING

For the intelligent robot for back-slap sputum excretion, the robotic arm is its most important motion actuator, and the back-slap sputum excretion terminal mounted on it will directly contact the human body during exercise. According to the actual operation of the care staff during the manual back-slap sputum excretion operation, it is necessary to slap the patient's back in a continuous order, at a uniform speed, and vertically when performing the back-slap sputum excretion care. According that, in order to better use the robotic arm to complete the back-slap sputum excretion of patients, we have designed the robotic arm motion planning method.

A. End Posture Supplement of Robotic Arm

Considering the practical application scenarios of the intelligent robot for back-slap sputum excretion, we need to install a back-slap sputum excretion terminal at the end of the robotic arm. In order to be closer to the effect of the care staff holding the expectoration machine terminal, we need to reduce the rotation of the terminal around the z-axis direction as much as possible when supplementing the posture of the robotic arm, and avoid large rotation, so as to improve the reliability of the intelligent robot for back-slap sputum excretion at work. Reflected in the robotic arm we use, the drive shaft of the back-slap sputum excretion terminal is always perpendicular to the

ground by means of the joint at the end of the robotic arm. Figure 12 is the schematic diagram of the AUBO robotic arm.

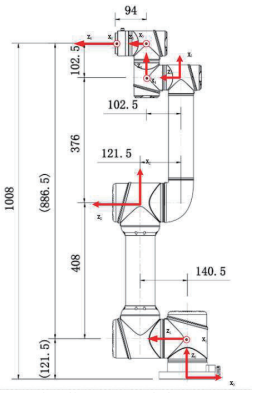

Figure 12. Schematic diagram of the AUBO robotic arm.

The position information of the robotic arm can be obtained according to the position points in the camera coordinate system and the posture transformation matrix between the camera and the basic coordinate system:

$$p_B = R_C^B p_C + T_C^B \tag{2}$$

Where R_C^B is the rotation matrix from the camera coordinate system to the base coordinate system, T_C^B is the translation vector from the camera coordinate system to the base coordinate system, p_B is the position in the base coordinate system, and p_C is the position in the camera coordinate system. Since the normal direction does not need to be translated, the posture information of the robotic arm is obtained according to the normal vector in the camera coordinate system and the rotation matrix between the camera and the base of the robotic arm:

$$p_{nB} = R_C^B p_{nC} \tag{3}$$

Among them, p_{nB} is the normal vector in the base coordinate system, and p_{nC} is the normal vector in the camera coordinate system. To describe the posture of the end, we need to provide the parameters that could form a completely coordinate axis. However, existing provided normal direction only constrains the orientation of the z-axis. It would constrain the spin angle around the z-axis and result in a non-unique end posture which requires us to supplement the posture of the end. The x-axis and y-axis of the robotic arm's end posture can be supplemented according to the following formula:

$$x_e = \begin{bmatrix} 0 \\ 0 \\ 1 \end{bmatrix} \times z_e \tag{4}$$

$$y_e = z_e \times x_e \tag{5}$$

The x-axis of the coordinate system formed in this way would be parallel to the xoy plane of the base coordinate system, it can ensure a relatively stable posture after installing the actuator at the end. Thus, we unitize the three coordinate axis directions to form a rotation matrix:

$$R_E^B = \begin{bmatrix} \frac{x_e}{|x_e|} & \frac{y_e}{|y_e|} & \frac{z_e}{|z_e|} \end{bmatrix} \tag{6}$$

In this way, the rotation matrix can be used to provide the Euler angle or quaternion required for the control of the robotic arm.

B. *Robotic Arm Motion Planning*

When the care staff performs the back-slap sputum excretion operation, the movements need to be relatively uniform and coherent. For the intelligent robot for back-slap sputum excretion, in order to better simulate the care staff`s manual operation strategy, multiple trajectory points are often required to move continuously, and combinate linear trajectory and arc trajectory to achieve smooth movement of complex trajectories. For the convenience of description, a plane four-way point motion scene is taken as an example here, as shown in figure 13. If only the linear trajectory planning is performed independently between each two waypoints, the robotic arm will not move smoothly due to sudden changes in the direction, speed, and acceleration of the robotic arm when passing through the middle waypoint.

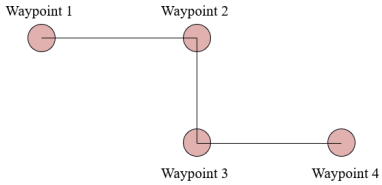

Figure 13. Waypoint planning for straight path.

Thus, we need to synthesize all the waypoint information for smooth trajectory planning. The main implementation of the existing robotic arm is to smooth the movement at the waypoint by setting the blend radius, as shown in Figure 14. At waypoint 2 and waypoint 3, circular trajectories are used to replace the original right-angle trajectories. The intermediate pose at the arc is approximately determined by the pose of the corresponding waypoint. Judge when to use arc trajectory planning according to the circle set at the waypoint, the robotic arm moves according to the trajectory of linear interpolation outside the circle, and the trajectory part in the circle performs arc interpolation based on two points on the circumference. The radius of the circle is blend radius[14].

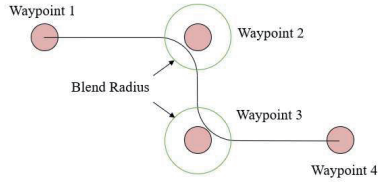

Figure 14. Waypoint planning with blend radius.

The trajectory movement realized by blend radius cannot accurately move to the position of the middle waypoint. However, for the intelligent robot for back-slap sputum excretion, the middle waypoint can be allowed to have a small deviation, and the end can be corrected by the force/position control method. After the deviation of the direction, the defects of this method can be effectively compensated.

In the actual working process of the robotic arm, the end of the robotic arm first moves to a position above the normal line of the first maker, and then pushes the back-slap sputum excretion terminal along the normal direction to contact the human`s back. In this way, it can be ensured that the back-slap sputum excretion terminal can fit the human`s back curve from the beginning to perform back-slap sputum excretion operation. Figure 15 is a schematic diagram of a complete back-slap sputum excretion operation cycle.

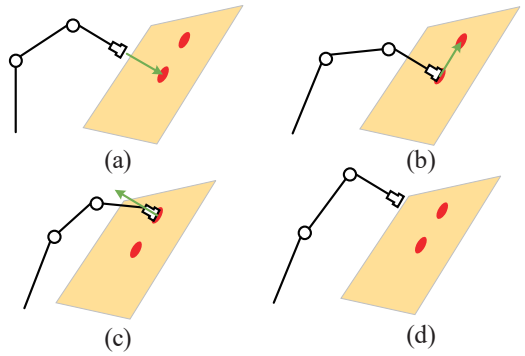

Figure 15. Schematic diagram of a complete back-slap sputum excretion operation cycle.

Among them, the robotic arm first runs to a distance above the normal line of the first maker (as shown in Figure 15(a)), and then vertically touches the human`s back (as shown in Figure 15(b)). Then perform a profile modelling on the human`s back, the back-slap sputum excretion terminal carried at the end of the robotic arm keeps in contact with the actual contour of the human`s back and moves to the end point. Afterwards, the end of the robotic arm is lifted along the normal direction of the end point (Figure 15(c)), and finally a cycle of back-slap sputum excretion is completed (Figure 15(d)).

V. EXPERIMENT

In order to verify the effectiveness of the back feature recognition method, we tested the method with the intelligent robot for back-slap sputum excretion. During the test, we designed the basic force/position control for the robot arm to ensure the safety of the user. Figure 16 is a flow chart of the robot performing a back-slap sputum excretion operation.


Figure 16. Flow chart of the robot performing a back-slap sputum excretion operation.

In the experiment, the intelligent robot for back-slap sputum excretion can follow the path points marked by the makers to perform a profile modelling on the patient's back and perform back-slap sputum excretion operations. From the experimental results we can see that the back feature recognition method based on markers designed in this paper can meet the basic needs of back-slap sputum excretion.

VI. CONCLUSION

This paper designed an intelligent robot for back-slap sputum excretion based on back feature recognition which can realize the automatic back-slap sputum excretion care of patients through effective recognition of the patient's back features. We verified the effectiveness of the robot in application through field experiments. In the future, we will further optimize related algorithms and design unmarked back feature recognition algorithms to improve the adaptability of this type of equipment in practice.

ACKNOWLEDGMENT

This work was financially supported by the National Key Research & Development Program of China (2021YFC0122700).

REFERENCES

[1] WHO, WHO Coronavirus (COVID-19) Dashboard, Available at: *https://www.who.int/emergencies/diseases/novel-coronavirus-2019*.
[2] Q.Y. Li, Y.Q. Chen, *Intensive Specialist Care*. People's Medical Publishing House:Beijing, 2018.
[3] IFR Statistical Department, World Robotics 2020 Service Robots, Available at: *https://ifr.org*.
[4] D.F. Zhang, T.M. Wang, J.H. Liu, et. "Research and Design of Task Flow of Traditional Chinese Medicine Massage Robot Based on Task Flow," *Robotics and applications*, vol. 1, pp. 23-27, 2012.
[5] S.Y. Lu, H.B. Gao, C.G. Liu, et al. "Design of Chinese medical massage robot system," in *2011 International Conference on Electrical and Control Engineering*, Yichang, 2011, pp. 3882-3885.
[6] G.Y. Du, S.Y. Lu, H.K. Zhang, "The Design of Searching Bodies` Acupuncture Point for Chinese Massage Robot," *Bulletin of Science and Technology*, vol. 27, no.5, pp. 637-640, 2011.
[7] R.C. Luo, S.Y. Chen, K.C. Yeh, "Human body trajectory generation using point cloud data for robotics massage applications," *2014 IEEE International Conference on Robotics and Automation (ICRA)*, HongKong, 2014, pp. 5612-5617.
[8] A.C. Dometios, X.S. Papageorgiou, C.S. Tzafestas, et al. "Towards ICT-Supported Bath Robots: Control Architecture Description and Localized Perception of User for Robot Motion Planning," *24th Mediterranean Conference on Control and Automation (MED)*, Athens, 2016, pp. 713-718.
[9] A.C. Dometios, X.S. Papageorgiou, A. Arvanitakis, et al. "Real-time end-effector motion behavior planning approach using on-line point-cloud data towards a user adaptive assistive bath robot," *2017 IEEE/RSJ International Conference on Intelligent Robots and Systems (IROS)*, Vancouver, 2017, pp. 5031-5036.
[10] A.C. Dometios, Y. Zhou, X.S. Papageorgiou, et al. "Vision-based online adaptation of motion primitives to dynamic surfaces: Application to an interactive robotic wiping task," *IEEE Robotics and Automation Letters*, vol. 3, no.3, pp. 1410-1417, 2018.
[11] L.H.T. Nam, T.C. Toai, T.K. Phong, et al. "Conceptual Design of Massage Robot Using in Healthcare Therapy," *2018 4th International Conference on Green Technology and Sustainable Development (GTSD)*, Vietnam, 2018, pp. 63-67.
[12] Z.Y. Chen, R.H. Wu, Y.Y. Lin, et al. "Plant disease recognition model based on improved YOLOv5," *Agronomy*, vol. 12, no.2, pp. 365, 2022.
[13] M. Drmota, E.Y. Jin, B. Stufler, "Graph limits of random graphs from a subset of connected k-trees," *Random structures & algorithms*, vol. 55, no. 1, pp. 125-152, 2019.
[14] S. Moe, I. Schjølberg, "Real-time hand guiding of industrial manipulator in 5 DOF using Microsoft Kinect and accelerometer," *2013 IEEE RO-MAN*, Gyeongju, 2013, pp. 644-649.